

AD _____

Award Number: DAMD17-97-1-7143

TITLE: 3-D Digital Imaging of Breast Calcifications: Improvements
in Image Quality, and Development of Automated
Reconstruction Methods

PRINCIPAL INVESTIGATOR: Andrew D. Maidment, Ph.D.

CONTRACTING ORGANIZATION: Thomas Jefferson University
Philadelphia, Pennsylvania 19107

REPORT DATE: February 2000

TYPE OF REPORT: Annual

PREPARED FOR: U.S. Army Medical Research and Materiel Command
Fort Detrick, Maryland 21702-5012

DISTRIBUTION STATEMENT: Approved for public release;
distribution unlimited

The views, opinions and/or findings contained in this report are
those of the author(s) and should not be construed as an official
Department of the Army position, policy or decision unless so
designated by other documentation.

20010620 185

REPORT DOCUMENTATION PAGE

Form Approved
OMB No. 074-0188

Public reporting burden for this collection of information is estimated to average 1 hour per response, including the time for reviewing instructions, searching existing data sources, gathering and maintaining the data needed, and completing and reviewing this collection of information. Send comments regarding this burden estimate or any other aspect of this collection of information, including suggestions for reducing this burden to Washington Headquarters Services, Directorate for Information Operations and Reports, 1215 Jefferson Davis Highway, Suite 1204, Arlington, VA 22202-4302, and to the Office of Management and Budget, Paperwork Reduction Project (0704-0188), Washington, DC 20503

1. AGENCY USE ONLY (Leave blank)		2. REPORT DATE February 2000	3. REPORT TYPE AND DATES COVERED Annual (15 Aug 97 - 14 Jan 00)	
4. TITLE AND SUBTITLE 3-D Digital Imaging of Breast Calcifications: Improvements in Image Quality, and Development of Automated Reconstruction Methods			5. FUNDING NUMBERS DAMD17-97-1-7143	
6. AUTHOR(S) Andrew D. Maidment, Ph.D.				
7. PERFORMING ORGANIZATION NAME(S) AND ADDRESS(ES) Thomas Jefferson University Philadelphia, Pennsylvania 19107 E-MAIL: maidment@esther.rad.tju.edu			8. PERFORMING ORGANIZATION REPORT NUMBER	
9. SPONSORING / MONITORING AGENCY NAME(S) AND ADDRESS(ES) U.S. Army Medical Research and Materiel Command Fort Detrick, Maryland 21702-5012			10. SPONSORING / MONITORING AGENCY REPORT NUMBER	
11. SUPPLEMENTARY NOTES This report contains colored photos				
12a. DISTRIBUTION / AVAILABILITY STATEMENT Approved for public release; distribution unlimited				12b. DISTRIBUTION CODE
13. ABSTRACT (Maximum 200 Words) In our work to date, we have generated a manually segmented and paired dataset of 110 patients images, which we have used as a "gold standard" in the evaluation of computer algorithms for identifying, segmenting and correlating calcifications. We have been able to develop two separate computer algorithms, one for identification and segmentation of potential calcifications, the other to find calcification triplets that should be paired. Both algorithms are quite robust. There are a number of significant findings from this work that will be published. First, the use of Euler's number to determine connectivity in an automated fashion is unique. Secondly, the simultaneous correction of patient motion and the determination of correspondence between the views is unique, and will be published. At this time, the algorithms are as good as the human observer. However, it now appears that the algorithm could be relatively easily improved. Similarly, the comparison to the human observer can be improved.				
14. SUBJECT TERMS Breast Cancer, Digital Mammography, 3-D Breast Imaging, Computer-Aided Diagnosis, Limited-View Image Reconstruction				15. NUMBER OF PAGES 31
				16. PRICE CODE
17. SECURITY CLASSIFICATION OF REPORT Unclassified	18. SECURITY CLASSIFICATION OF THIS PAGE Unclassified	19. SECURITY CLASSIFICATION OF ABSTRACT Unclassified	20. LIMITATION OF ABSTRACT Unlimited	

NSN 7540-01-280-5500

Standard Form 298 (Rev. 2-89)
Prescribed by ANSI Std. Z39-18
298-102

FOREWORD

Opinions, interpretations, conclusions and recommendations are those of the author and are not necessarily endorsed by the U.S. Army.

N/A Where copyrighted material is quoted, permission has been obtained to use such material.

N/A Where material from documents designated for limited distribution is quoted, permission has been obtained to use the material.

N/A Citations of commercial organizations and trade names in this report do not constitute an official Department of Army endorsement or approval of the products or services of these organizations.


N/A In conducting research using animals, the investigator(s) adhered to the "Guide for the Care and Use of Laboratory Animals," prepared by the Committee on Care and use of Laboratory Animals of the Institute of Laboratory Resources, national Research Council (NIH Publication No. 86-23, Revised 1985).

X For the protection of human subjects, the investigator(s) adhered to policies of applicable Federal Law 45 CFR 46.

N/A In conducting research utilizing recombinant DNA technology, the investigator(s) adhered to current guidelines promulgated by the National Institutes of Health.

N/A In the conduct of research utilizing recombinant DNA, the investigator(s) adhered to the NIH Guidelines for Research Involving Recombinant DNA Molecules.

N/A In the conduct of research involving hazardous organisms, the investigator(s) adhered to the CDC-NIH Guide for Biosafety in Microbiological and Biomedical Laboratories.

 3/29/01

PI - Signature Date

Table of Contents

Cover.....	1
SF 298.....	2
Table of Contents.....	4
Introduction.....	5
Body.....	6
Key Research Accomplishments.....	17
Reportable Outcomes.....	18
Conclusions.....	20
References.....	20
Appendices.....	21

1. Introduction

An automated technique has been developed and evaluated to reconstruct 3-D binary images of breast calcifications. The reconstruction algorithm consists of segmentation, motion correction, correlation between views, 3-D binary limited-view reconstruction of each calcification, and 3-D rendering.¹ This method relied upon significant human intervention and judgment in producing the final 3-D image. In this grant, we sought methods to automate these tasks. Required were robust methods of identifying, segmenting and correlating (or pairing) calcifications between views.

The tasks of identifying and segmenting calcifications have been attempted on numerous occasions. These previous attempts have been used almost exclusively in computer aided diagnosis (CAD) systems. In such systems, the desire is to capture a sufficient number of calcifications to identify clusters of suspicious calcifications for evaluation by a human observer. Significant effort is expended on eliminating false positives. By imaging the breast at 3 separate angles with known spatial alignment, we have the advantage that true calcifications are present in each of the images, while most spurious or non-calcified signals are found in only one image. This additional constraint allows us to segment more calcifications in each image, admittedly with a high false positive rate. The task of correlation between the images quite naturally reduces the false positive rate in the 3-D image.

The work to date is reviewed in this annual report.

2. Body

2.1. Summary of Work Items

It is useful to restate the work items listed in the original grant. They are as follows:

- Task 1: Compile database of 50 selected cases (Months 1-2)
- Task 2: Manually identify and pair calcifications in database images (Months 3-4)
- Task 3: Evaluate methods for automated identifications, segmentation and correlation of calcifications (Months 1-24)
- Task 4: Apply reconstruction technique to non-calcified structures (Months 25-36)

At the current time, tasks 1 & 2 are complete and task 3 is essentially complete. A decision must soon be made as to whether the remaining time should be used to refine the results of tasks 1-3 or to undertake task 4. It is the preference of the PI to perform this refinement. However, the opinion of the DOD Program Director will be sought prior to any change in work items. In the following report, a discussion of the accomplishments for the period of October 1, 1997 until March, 2001 will be provided. Due to extensions and delays incurred during the performance of this grant, a detailed summary of the timeline of events affecting this grant will also be offered.

2.2. Database Formation

We were able to obtain image data on 130 women from two different prior studies. Both studies were conducted under IRB review. The first (TJU IRB control #93.0705) consisted of a retrospective review of images from 74 patients who had had a stereotactic core biopsy for breast calcifications, or of breast tissue specimens containing calcifications. In the latter case, the specimens had been imaged in a water bath to simulate breast tissue of equal thickness to a normal breast. However, as we shall discuss below, these latter images lack the complexity of background structures that are found in real mammograms. The second study (TJU IRB control #96.0160) was a prospective study of women having core breast biopsies. The DOD funded this latter study.¹

For each patient, three images of the breast were obtained at $\pm 15^\circ$ of separation. Of the patient's images in the database, 10 were of specimens, while the remainder was acquired *in vivo*. Of the 130 cases, 42 were malignant (32.3%). A summary of the patient race is given in Table 1. The racial distribution is similar to our patient population as a whole.

Table 1: Summary of Patient Race of the Image Database

IRB Control #	White	Black	Asian/ Oriental	Other	Unknown	Total
93.0705	59	11		1	3	74
96.0160	43	6	1		6	56
Total	102	17	1	1	9	130

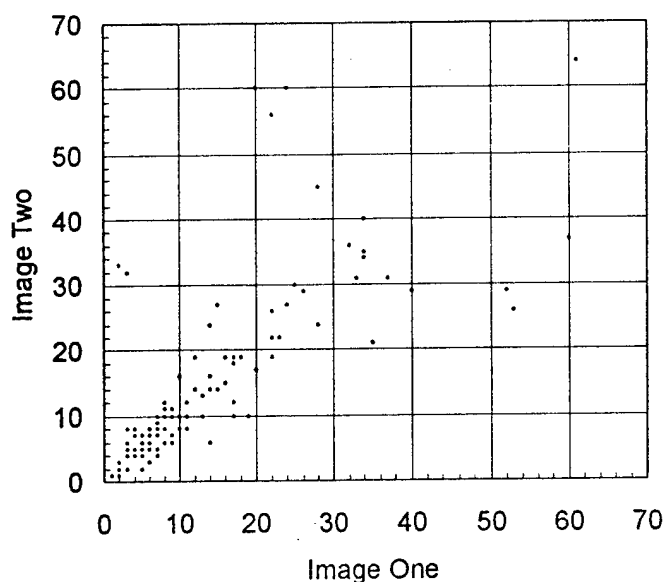


Figure 1 Comparison of the number of calcifications that were manually segmented from each view of the same patient

2.3. Manual Evaluation of Images

Two skilled observers evaluated the images in the database. The first observer performed manual segmentation and correlation of 47 images. The second observer manually segmented and correlated calcifications in 110 cases. Later, that same observer re-evaluated the same images and segmented all visible calcifications that could not be paired manually. Note that 20 cases were eliminated for a number of reasons, including withdrawal from the study, insufficient numbers of radiographically visible calcifications, and lack of radiographically visible calcifications.

The consistency of the image data was tested by comparing the number of calcifications segmented by a human observer in two views of each of 110 cases. In this experiment, all visible calcifications were segmented, not just those that could be paired. Figure 1 shows the number of segmented calcifications between two images for each case. 4 clusters had in excess of 70 calcifications. Linear correlation coefficient is 0.848. On average, 15.9 calcifications were identified per image, and 8.7 calcifications were paired per image (55%).

A comparison of the reconstructed images of 47 cases, generated by the two different operators, was used to assess the inter-operator variability of the reconstruction method, and to determine the validity of the manually segmented image data. Shown in figure 2 is the correlation between the two operators for the number of segmented pairs of calcifications. Agreement in segmenting individual calcifications occurred in 81% of calcifications, and agreement of pairing calcifications occurred in 70% of pairs. Linear correlation coefficient of plotted data is 0.993.

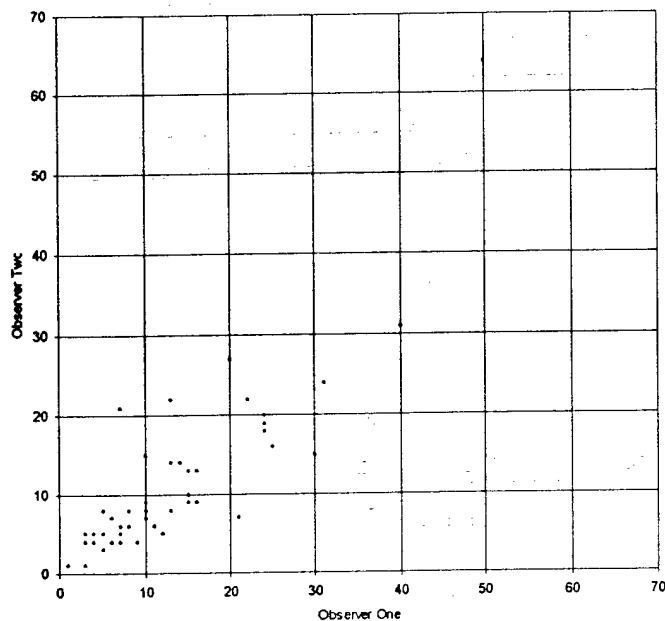


Figure 2 Interoperator variability of segmentation and correlation of calcifications is shown, by comparing the number of paired calcifications found in each image.

In summary, a data set of 130 cases was obtained. For the purposes of testing the algorithms for identification, segmentation and correlation of calcifications, 110 patient's images were used. It should be noted that in some of the work discussed below, we also found it necessary to eliminate the 10 cases that consisted of specimen images. In these instances, the calcifications were too obvious. This is due mainly to the lack of overlaying tissues that would otherwise confound discovery and reduce conspicuity of the calcifications.

2.4. Automated Identification and Segmentation

The algorithm first proposed in the grant application was found to be inadequate. The initially proposed method involved wavelet processing of the images. However, unfortunately, the algorithm was not intuitive; instead it relied upon operational parameters that had no physical basis. As a result, while it was capable of segmenting large numbers of calcifications, it could not be easily tuned, and it was similarly difficult to differentiate those objects it had segmented. For this reason, we rethought the segmentation approach and developed a new algorithm. This algorithm has the benefit of being physical. It also has the advantage that it can be tuned to aggressively segment potential calcified regions. Thus, we can rely upon the correlation step to distinguish between artifactual and actual calcifications.

The algorithm proceeds as follows. First, large-scale trends are removed from the image using an unsharp mask with a 31x31 kernel. Next, spurious signals are eliminated by performing statistical analyses of 5x5 neighborhoods and eliminating points greater than 3 times the population variance. A Laplacian operator is applied on 7x7 regions, and then calcifications are selected based upon a local threshold on these data.

The segmentation is based upon a heuristic illustrated below in figures 3 & 4. Rather than compute the number of connected regions as a function of threshold, we calculate a connectivity factor based upon Euler's formula

$$C(t) = F(t) - E(t) + V(t)$$

where $V(t)$ is the number of sample points (vertices) below the threshold, $E(t)$ is the number of pairs of vertically or horizontally adjacent points (edges), and $F(t)$ is the number of groups of 4 pixels (faces) in the form of a square. We have found experimentally that a threshold of 25% of the maximum connectivity value is optimal.

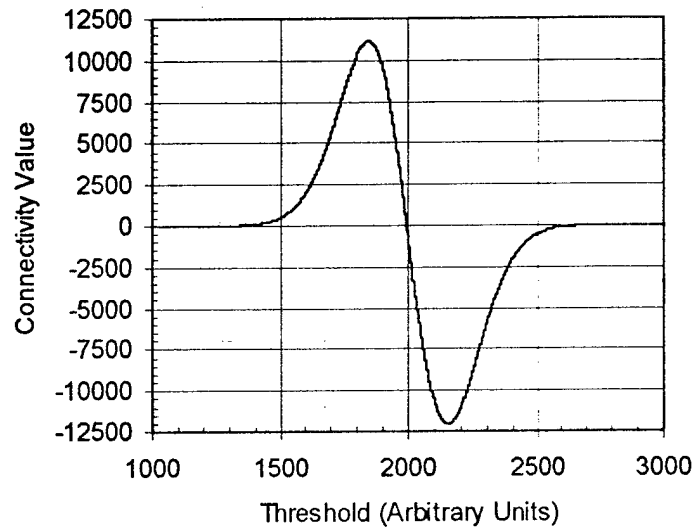


Figure 3 An example of the connectivity calculation applied to one of the images from the database. The optimal threshold occurs at 25% of the maximum connectivity value.

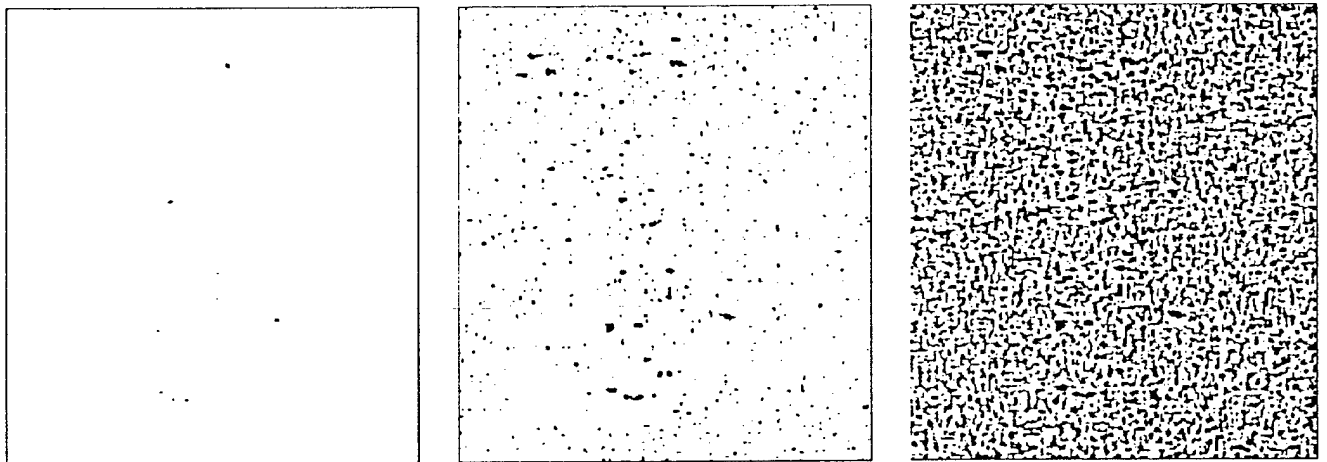


Figure 4 An example of how connectivity varies as a function of threshold. The leftmost image has a threshold which is too low, the middle is appropriate (this threshold is determined by the point on the connectivity graph where the connectivity factor is 25% of the maximum value), and the rightmost is too high.

We next eliminate obvious false positives. Calcifications within 20 pixels of the edge of the image are eliminated, as are those containing fewer than 4 pixels ($100 \mu\text{m}^2$). We also test calcifications in terms of contrast. By defining a region extending 7 pixels beyond the edge of the segmented structure, we can calculate a signal-to-noise ratio. If this ratio is less than 5, then the calcification is eliminated. Finally, calcifications associated with long linear structures, such as blood vessels are eliminated. An example of the complete method is illustrated in figure 5.

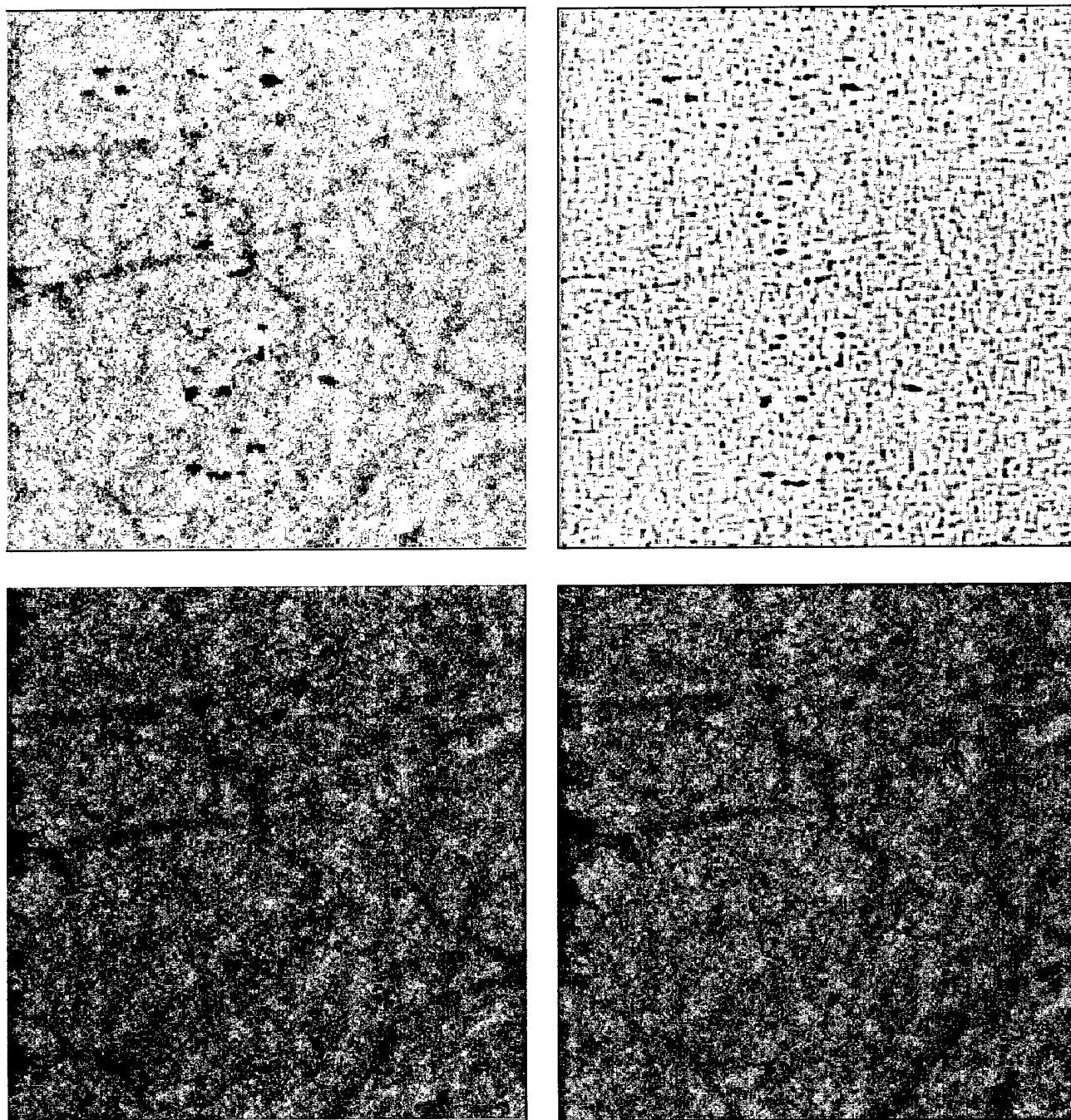


Figure 5 An example of the complete segmentation process. (upper left) An image after large scale trends and spurious signals have been eliminated, (upper right) the same image is shown after the 7×7 Laplacian operator is applied, (lower left) image obtained by applying the 25% threshold - at this point many false positive signals still exist, and (lower right) the final output of the segmentation process.

Shown in figure 6 is the number of calcifications that were automatically segmented in each image compared to the two other images in each patient's dataset. On average, 57.7 calcifications were segmented per image (min 16, max 203) in an analysis of 109 cases (327 images). The linear correlation coefficient is 0.777. There is no correlation between the number of calcifications seen and the specific viewing angle. The average number of calcifications seen was 56.3, 57.8 and 59.0 for the three different views. This number is approximately 4 times that found by the human observer. However, a significant number are false positives.

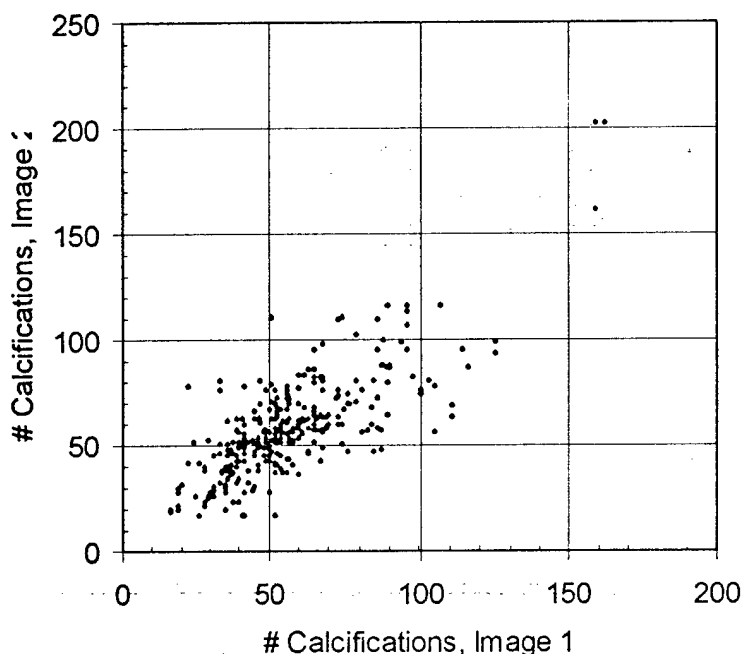


Figure 6 Correlation of the number of calcifications segmented between any two of the three views used to reconstruct the calcifications

A scatter graph of the minima of the number of calcifications segmented in the three 2-D source images for each of 110 cases and the number of calcifications paired in 3-D from those views is shown in figure 7. The minimum of the number of calcifications in the 3 images was on average 49.1, as compared to an average number of calcifications of 57.7. Of these, on average 8.78 were paired (16.3%). The data can be fit to a line of the form $y = 0.346x - 8.18$. The correlation coefficient is 0.772, and the x-intercept is 23.6.

The number of calcifications correlated by the algorithm matches the number paired by the human observer. However, there are a number of differences that should be noted. First, there was agreement between the human and the machine in about $\frac{1}{2}$ of the cases. This is not, in and of itself, a reason for concern, as there are a number of differences in the approaches used. For instance, the machine matched calcifications in 3 views, while the human only matched calcifications in 2 views. There were definitely calcifications that were only seen in 2 of 3 views. Methods of improving these results are discussed in Section 5.6

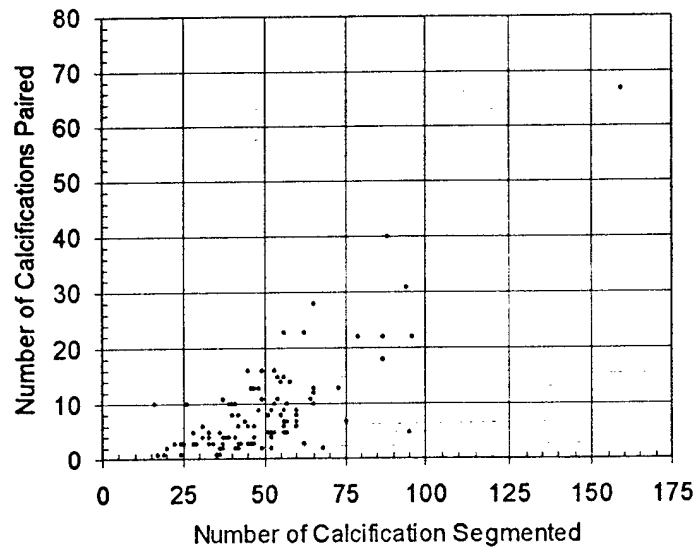


Figure 7 Correlation between the minimum number of calcifications segmented in the three source images and the number of calcifications paired for the same case

Automated Correlation

As shown in figure 8, a calcification falls on a line between the image of the calcification and the x-ray focal spot. Given two views, their intersection should give the location of the calcification; a third view is redundant. Realistically, the lines are skew due to patient motion, the finite size of the image, and uncertainty in the acquisition geometry.

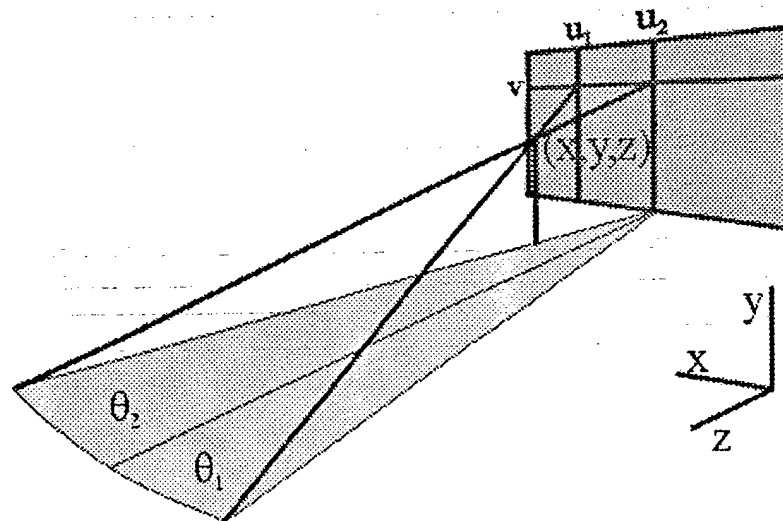


Figure 8 Geometry of image acquisition, showing the general problem of imaging a calcification from 2 views.

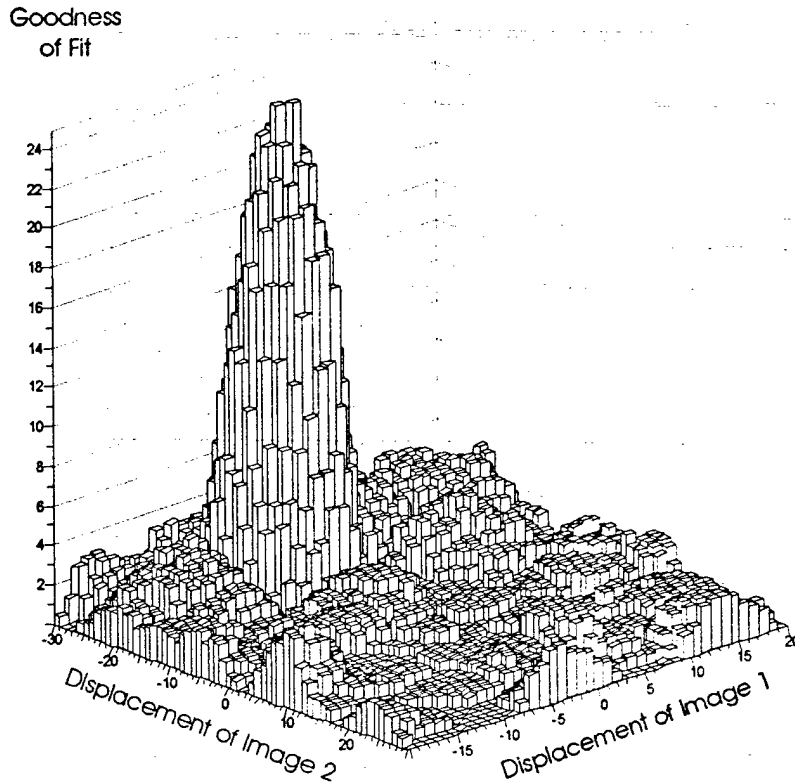


Figure 9 An example of the goodness of fit calculation for a set of displacements in two of the three images. Such calculations were performed to account for patient motion and the imprecision of the motion of the x-ray tube arm. The goodness of fit criterion is determined from the number of calcification triplets that can be paired with sufficient proximity.

We simultaneously solve the correspondence problem and the geometry problem. We assume that geometric uncertainty can be compensated for by shifts of the second and third images. For each shift, a count is made of the number of triples whose positions are consistent with being in the shadow of a single calcification. The parameter space of shifts is searched to maximize the count.

For each possible triplet, the calcification position is found by minimizing the sum of the squares of the distances to the three lines. The sum, χ^2 , for each possible triplet is sorted in ascending order, such that each calcification shadow is used uniquely. The sum of $1/(1+(\chi^2/\sigma^2)^2)$ is calculated over these triplets. The result is 1 if the three shadows are perfectly aligned and becomes 0 if the lines are highly skew. The value of σ^2 is related to the distance between the best-fit point and the lines for shadows which are consistent. For this work σ^2 is such that the distance of best fit is 50 μm . An example of the fitting process (in a restricted 2-D subspace) is shown in figure 9.

We are not aware of a previous attempt to use such a metric to correct for motion or determine correspondence in similar algorithms applied to computer-based vision. This is one of the most significant pieces of new work in this grant, and is being written up as a scientific paper.

2.5. Discussion and Summary of Scientific Results

In our work to date, we have generated a manually segmented and paired dataset of 110 patients images, which we have used as a "gold standard" in the evaluation of computer algorithms for identifying, segmenting and correlating calcifications. We have been able to develop two separate computer algorithms. Both are quite robust. There are a number of significant findings from this work that will be published. First, the use of Euler's number to determine connectivity in an automated fashion is unique. Secondly, the simultaneous correction of patient motion and the determination of correspondence between the views is unique, and will be published. At this time, the algorithms are as good as the human observer. However, it now appears that the algorithm could be relatively easily improved. Similarly, the comparison to the human observer can be improved.

There are two potential flaws with the existing work. First, the segmentation and pairing by the human observer could be better. We have found that it is significantly easier to identify and pair calcifications in images that have had all low-frequency details removed. This is essentially the first step of our automated process. We propose to reanalyze the images by a human observer following processing of the images with a 31x31 unsharp mask. This step would make the search task easier, and hence a larger number of calcifications would be found, and a larger number could be paired.

The second flaw is with the correlation step. Currently, we only correlate findings seen in all three images. We now realize that there are calcifications that are only visible in two images. We would like to use the motion correction that is determined in the first step of 3-view correlation to then be applied to 2-view correlations between the 3 possible pairs of images. We believe that this will result in more calcifications being correlated between views by the computer. We also believe that this will result in better agreement between the computer and the human observer.

The original intent of task 4, was to add features to the image that would add perspective to the calcification images. At this time, it is not clear what those features would be. Faced with the choice between preceding with work item #4, and refining the work to date for items 1-3; I, as the PI, would prefer to continue to work on the refinement. I believe that this is the best use of resources and the most likely to have a beneficial effect in the long term. The 3-D images produced by this method are best when many calcifications are segmented and correlated. Expending effort on maximizing this number is better than tackling new and unknown problems.

2.6. Discussion of Administrative Issues

Significant progress has occurred with this grant, and a successful conclusion is likely in the near future. However, it is useful to discuss the timeline and events that have shaped the life of this research project. When first proposed, the work was to be performed by Andrew Maidment (PI), Michael Albert (research assistant), and Emily Conant (clinical collaborator). Two additional radiologists, and a pathologist were included to provide additional clinical assistance when necessary. Prior to beginning the grant Dr. Conant left Thomas Jefferson University. This was a major loss as Dr. Conant, among all of the radiologists at Thomas Jefferson University Hospital, was most familiar with the project and had previously contributed most to the project. We have never since had a radiologist with her clarity of insight into this clinical problem.

Next, since the departure of Dr. Conant, we have had a number of additional people start and leave the TJUH breast center, including Dr. Stephen Feig, Dr. Dionne Farria, Dr. Jane Hughes, Dr. Stephen Lee, Dr. Steven Nussbaum, Dr. Barbara Cavanaugh, and others. This has had a negative impact on all of the research being performed at the breast center. Dr. Catherine Piccoli assumed Dr. Conant's responsibilities, as was communicated to the DOD. In addition, Dr. Feig and Dr. Farria did work on this grant briefly.

As related in Dr. Maidment's letter dated June 3, 1999, a waiver of the 1998 report and a one-year no cost extension were requested due to the clinical load of Dr. Maidment and Dr. Albert. Prior to that date, Drs. Maidment and Albert were expending essentially 100% of their time in support of clinical medical physics and PACS at Jefferson. Prior to this time, no salary was drawn from the grant. The department acknowledged these issues, in part, and hired 2 people to assume some of Dr. Maidment's and Dr. Albert's clinical responsibilities. In neither case, has this replacement been complete. As a result Dr. Maidment still spends at least 40% of his time clinically, and Dr. Albert spends at least 30% of his time clinically. Thus, while significant progress has occurred since June of 1999, the work is not complete. As such, task 4 has not yet been started.

At the same time, our progress in Tasks 1-3 has given us additional insight that we did not previously possess. For example, we now know which types of cases are best suited to this type of image reconstruction. We have a better understanding of what makes the 3-D rendering useful to different doctors (partly from our work in the related grant¹). We are now at a point where given a seed location for a calcification, we can virtually always segment it. We can also determine correspondence with better accuracy using the computer than with humans (a retrospective analysis of computer generated correspondences actually made us question the work of the human observer). We also know that the correlation would be improved if we could pair calcifications in 2 views (there are 3 sets of pairs we can use in each case). We would only do this last step after obtaining all possible triplets.

For this reason, we would like to recommend the following. We request the input of the program office of the DOD. First, we would like to extend the completion date of the grant by an additional year. Although we will not need the full year to complete the

work, it will allow us addition time to prepare this work for publication. A formal request for the extension will be send to the DOD shortly.

Secondly, the exciting results to date have left us highly motivated to proceed, in this last year of the grant, to refine the work in tasks 1-3, rather than proceed with Task 4. Namely, we wish to reanalyze the images manually, first applying some of the image pre-processing steps from the automated analysis. This, we have observed, makes the calcifications easier to find, as they are more obvious in their appearance. We also wish to add pair-wise calcification correlation after having searched for triplets. This overcomes the problem that some calcifications are only seen in two of three images. By performing the triplet analysis first, we can apply motion corrections prior to pairing. Finally, we would like to test the correlation analysis differently. We will do this by having human observers judge the accuracy of each computer generated pairing on a multipoint scale. This will better allow us to determine the performance of the algorithm. Again, we would appreciate the opinion of DOD in this matter, and seek your permission to alter the proposed work as outlined above.

3. Key Research Accomplishments

The following is a list of key research accomplishments resulting from this work:

- Developed a database of 110 biopsy-proven cases, with 3 digital images of each case
- Developed a set of segmented images from each of 110 cases. In these data, each calcification from all three views of each patient was manually identified, and semi-automatically segmented.
- Developed a set of manually determined correspondences.
- These datasets were used to develop an automatic identification and segmentation algorithm that tested each point in an image as a potential seed point and then tested each resultant segmented region for validity as a potential calcification. A key feature of this algorithm was the use of Euler's number to determine connectivity.
- The above datasets were also used to develop an automatic correspondence algorithm. The algorithm used a weighted summation that allowed us to simultaneously correct for patient motion and determine optimal correspondence.

4. Reportable Outcomes

a) Published Manuscripts

A.D.A. Maidment, M. Albert, and E.P. Conant. Three-Dimensional Imaging of Breast Calcifications. In *Exploiting New Image Sources and Sensors*. Proceedings of the SPIE, 3240, 200-208 (1997).

A.D.A. Maidment, M. Albert, E.F. Conant, and S.A. Feig. Three-Dimensional Visualization of Breast Cancer. In *Digital Mammography '98*, edited by N. Karssemeijer, M. Thijssen, J. Hendricks, and L. van Erning, Kluvier, Holland, 57-60, (1998).

A.D.A. Maidment, and M. Albert. "Automated Reconstruction of 3-D Calcifications". In *Digital Mammography 2000*, In press, 2001.

b) Abstracts and Presentations

A.D.A. Maidment, M. Albert, E.F. Conant, and C.W. Piccoli. A method for three-dimensional imaging of breast calcifications. World Congress on Medical Physics and Biomedical Engineering, Nice, France, Sept. 18, 1997. (Poster)

A.D.A. Maidment, M. Albert, E.F. Conant, and C.W. Piccoli. A method for three-dimensional imaging of breast calcifications. Medical and Biological Engineering and Computing, 35, Supplement Part 2, 751 (1997).

A.D.A. Maidment, M. Albert, E.F. Conant, S.A. Feig, C.W. Piccoli, S.A. Nussbaum, *et al.* A computer workstation for 3-D imaging of the breast. 83rd Scientific Assembly of the Radiological Society of North America, Chicago, IL, Nov. 30 - Dec. 5, 1997. (InfoRAD)

A.D.A. Maidment, M. Albert, E.F. Conant, S.A. Feig, C.W. Piccoli, S.A. Nussbaum, *et al.* A computer workstation for 3-D imaging of the breast. Radiology, 205(P), 741 (1997).

A.D.A. Maidment, M. Albert, and E.P. Conant. Three-Dimensional Imaging of Breast Calcifications. The 26th AIPR Workshop: Exploiting New Image Sources and Sensors, Cosmos Club, Washington DC, Oct. 16, 1997.

A.D.A. Maidment, M. Albert, E.F. Conant, and S.A. Feig. Three-Dimensional Visualization of Breast Cancer. 4th International Workshop on Digital Mammography, Nijmegen, The Netherlands, June 10, 1998.

A.D.A. Maidment, 3-D Imaging of the Breast. 6th International Cambridge Conference on Breast Cancer Screening. Cambridge, England. April 14, 1999.

A.D.A. Maidment, and M. Albert. "Automated Reconstruction of 3-D Calcifications". 5th International Workshop on Digital Mammography, Toronto, Canada, June 14, 2000.

A.D.A. Maidment. "3-D Imaging of the female breast". Imaging 2000, Stockholm, Sweden, June 29, 2000. (Invited Presentation)

A.D.A. Maidment, and M. Albert. "Automated 3-D Limited-View Binary Reconstruction of Breast Calcifications". 42nd Annual Meeting of the American Association of Physicists in Medicine, Chicago, IL, July 25, 2000.

A.D.A. Maidment, and M. Albert. "A Clinical Study of Calcifications Imaged by 2-D and 3-D Digital Mammography". DOD Era of Hope, Atlanta, GA, June 8-11, 2000.

A.D.A. Maidment, and M. Albert. "3-D Digital Mammography: An Automated Method of Image Reconstruction". DOD Era of Hope, Atlanta, GA, June 8-11, 2000.

A.D.A. Maidment, P. Bakic and M. Albert. "3-D Digital Mammography: A Comparison of Image Reconstruction Methods". DOD Era of Hope, Atlanta, GA, June 8-11, 2000.

c) Funding Applications

Andrew D. A. Maidment, Principle Investigator, DOD Breast Cancer Research Grant, DAMD17-98-1-8159, "3-Dimensional Imaging of the Breast". 7/98 - 6/2001.

5. Conclusions

In conclusion, we have developed automated algorithms for identifying, segmenting, and correlating calcifications in 3-D, using 3 sources images acquired at 15 degree increments. The algorithms have been tested with previously acquired clinical data, which was arranged into a database, and was analyzed by human observers for the purpose of developing a gold standard for the reconstructions. The algorithms have worked very well. The use of Euler's formula for connectivity analysis and the simultaneous correction of image correlation and image motion are particularly noteworthy accomplishments. Further work remains, and will be performed in the next year.

With regard to the choice of future work, we are nearly complete the work originally proposed in Tasks 1-3. Task 4 is likely to prove difficult, and from the insight gained over the last few years, we believe that our effort would best be spent on further improving the algorithms, and on refining the metrics used to calculate the accuracy of the algorithms.

6. References

¹ DOD Grant DAMD 17-1-96-6280, A Maidment, PI, "XXXXXX"

7. Appendices

Attached to this report is a preprint of the paper written for the presentation by A.D.A. Maidment and M. Albert, entitled "Automated Reconstruction of 3-D Calcifications". This work was presented at the 5th International Workshop on Digital Mammography in Toronto, Canada on June 14, 2000.

AUTOMATED RECONSTRUCTION OF 3-D CALCIFICATIONS

Andrew D. A. Maidment and Michael Albert

Thomas Jefferson University, Philadelphia, PA, USA

Table of Contents

1. Introduction
2. Methodology
3. Results and Discussion

1. Introduction

Conventional mammography fails, in part, due to the processes of projection and superposition. These processes occur whenever a 2-dimensional image is produced from a 3-dimensional object. We have attempted to overcome this failing by producing 3-D images of breast calcifications to be used in the determination of malignancy. The rationale for this procedure have been discussed previously, as has a preliminary manual methodology.^{1,2} The results were sufficiently promising to justify additional work in automating the technique.

3-D images are generated using a limited-view binary reconstruction algorithm, with source images acquired from a stereotactic digital mammography system (typically, three images separated by 15° each). The initial method involved manually identifying calcification pairs between two images and subsequently reconstructing each calcification in 3-D from these projection data. In the automated method, candidate calcifications are determined in each view, then the correspondence between views is determined, and finally a reconstruction algorithm is applied to each calcification. In this paper, the segmentation and correspondence algorithms are described. These differ from the work of others (particularly those developed for CAD), in that

we are less concerned with false positive segmentations. We can rely upon the correspondence algorithm to exclude spurious objects that are segmented in only a single view, thereby reducing false negatives.

2. Methodology

The segmentation algorithm begins by producing a smoothed version of the image, formed by taking the median over 31×31 pixel regions, and subtracting this from the original image to remove large scale trends. An offset of 2000 is added to the pixel values for convenience. Next, to reject pixels containing spurious signals, the mean and population variances are computed in 5×5 pixel regions around each point (excluding the pixel being tested) and if the tested pixel differs from the population mean by more than 3 times the population variance, the pixel's value is replaced by the population average. This generally affects fewer than 5% of the pixels. An example is shown in figure 1. Note that in this paper, the calcifications are shown darker than the background, which is the opposite polarity from film.

The images are then subjected to a Laplacian on 7×7 pixel regions, in which the second-order derivatives are estimated in a least-squares manner, shown in figure 2. In the following, $I_{m,n}$ will represent the processed pixel values shown in figure 1 and $L_{m,n}$ will represent the negative of the Laplacian as shown in figure 2

Calcification candidates are selected based upon local thresholding of the Laplacian data. The threshold is set locally based upon the following algorithm. Consider the segmented image as a function of threshold. For a very low (restrictive) threshold, only the most obvious calcifications pass (figure 3). As the threshold is raised, more calcification candidates are identified (figure 4). However, if the threshold is raised too high, regions begin to merge and the threshold is no

longer useful for identifying calcifications (figure 5). Heuristically, it is clear that one wants to set the threshold in the intermediate range where there are many small regions, but below the point at which these regions merge into a few large regions.

Computing the number of connected regions, as a function of threshold is computationally intensive. Therefore, we calculate a connectivity factor based upon Euler's formula,

$$C(t) = F(t) - E(t) + V(t) ,$$

where $V(t)$ is the number of sample points (vertices) at which the pixel value is less than the threshold t , $E(t)$ is the number of pairs of horizontally or vertically adjacent points (edges) which are below the threshold t , and $F(t)$ is the number of groups of 4 pixels (faces) whose coordinates are of the form $\{(m,n),(m,n+1),(m+1,n),(m+1,n+1)\}$. The graph of this connectivity factor as a function of threshold is shown in figure 6 for the same image as in figure 1. For low values of the threshold, no pixels pass so $C(t)=0$. When only a few pixels pass, the connectivity factor is approximately equal to the number of connected regions that pass the threshold. The connectivity number reaches a maximum, and for sufficiently large values of t is equal to 1, because for large threshold t all pixels are accepted and the entire region of interest becomes one large segmented region. The value of $C(t)$, as defined, can become negative when connected regions contain holes, and indeed the behavior shown in figure 6 has been found to be typical of the mammographic images in our database. The optimum threshold is set to correspond to the value of t where $C(t)$ is a certain fraction of its maximum. This procedure is appealing because it provides a method of setting the threshold in which the identified candidates are independent of any monotonic remapping of the pixel values.

Various modifications of this procedure could be considered; for example, using region count instead of the connectivity number. The connectivity number has the advantage that the entire graph can be calculated in a single pass through the region of interest. In any case, for the values of threshold t of interest, the connectivity factor $C(t)$ approximates the number of connected regions. Experimentally we have found that setting the threshold to a value of t where $C(t)$ reaches 25% of its maximum produces good results. The connectivity graph is relatively stable for all regions in the image. However, to take into account local variations, the above procedure is performed for overlapping 250x250 pixel regions which cover the image. Thus, the resulting set of candidates is the union of the pixels identified by application of the procedure to each of the overlapping regions. In figure 7, the regions identified using the 25% threshold are shown in red superimposed on the same image as in figure 1.

Each connected region in figure 7 is now considered a calcification candidate, for which additional features are calculated to remove false positives. Any region within 20 pixels of the edge of the image or containing fewer than 4 pixels is removed. Further tests attempt to remove false positives based upon the contrast of the calcification candidate relative to the background and the possible association of the candidate with the shadow of a larger structure within the breast.

Two measurements of local contrast are calculated, based upon a quadratic fit in a neighborhood, N , of the calcification. For the purposes of this fit, those pixels identified as being in the candidate calcifications are excluded from N . To provide a small tolerance in the choice of threshold, pixels whose value $L_{m,n}$ falls below the 35% threshold determined from the $C(t)$ graph are excluded. Except for the pixels thus excluded, the region N is defined as a square extending

7 pixels beyond the candidate calcification in each direction. The goodness of the fit is estimated by the χ^2 per degree of freedom of the fit

$$\chi^2 = (1/(N-6)) \sum (I_{m,n} - f(m,n))^2$$

where the sum covers the N points used for the fit and $f(m,n)$ is the quadratic fit (which has six free parameters). The statistical significance of the signal can then be represented by the ratio of the value χ^2 calculated for the pixels in the candidate region to the χ^2 per degree of freedom used in the fit. If this ratio is less than 25 (SNR of 5) the candidate is rejected. Additionally, if the maximal depth of the candidate region relative to the quadratic fit ($\max(f(m,n) - D_{m,n})$ for (m,n) in the candidate region) is less than twice the square root of the χ^2 per degree of freedom of the fit, the calcification is rejected.

False calcification candidates with sufficient contrast to pass these tests are often associated with larger structures in the breast, as illustrated in figure 8. To test for association with a possible larger structure, an attempt is made to roughly segment these larger structures. Using a 300x300 pixel region, an estimate is made of the typical pixel-to-pixel variation

$$\sigma_{loc}^2 = \langle (I_{m,n} - I_{m,n+1})^2 \rangle + \langle (I_{m,n} - I_{m+1,n})^2 \rangle + \langle (I_{m,n} - I_{m+1,n+1})^2 \rangle.$$

Starting from the calcification, a region is grown to include all pixels with value $I_{m,n}$ σ_{loc} below the average. Figure 9 shows the approximate segmentation of these structures for the calcification candidates in figure 8. If the resulting region is larger than 1000 pixels, the region is rejected. If the maximum contrast is less than twice the population variance of the pixel values in the larger region, then the candidate is also rejected on the grounds that it is really a continuation of that region. Further, if the difference in the average value of the pixels inside the calcification candidate and the average of the pixel values in the larger segmented region

differ by less than the sum of the population variances for these two regions, the calcification is also rejected. If this difference is less than twice the population variance of the entire 300x300 region, the candidate is also rejected.

Additionally, some false positive calcification candidates are associated with distinctly linear features in the breast image, and these candidates can be highly elongated in the direction of this linear feature. To test for this, the two pixels in the calcification candidate whose inter-pixel distance is maximal are found. The line running through this is defined as the long axis of the calcification. The width of the candidate is then determined. If the ratio of the width to the length is less than 0.25, we attempt to locate a linear feature along the axis of the calcification. First, the maximal distance, d_{max} , of any pixel in the candidate from the long axis is found. Second, a square region of interest with side length three times the length of the calcification is identified. Three categories of pixels are identified: those between 2 and 4 times d_{max} on one side of the axis, those within d_{max} of the axis, and those between 2 and 4 times d_{max} on the opposite side of the axis. Pixels identified as being inside calcification candidates are excluded from these regions. If the average of the regions on both sides is greater than the average of the central region by more than 5 times the population variances of the regions, added in quadrature, this is taken as evidence that the candidate is actually part of a linear feature of the breast and rejected.

As shown in figure 10, this somewhat *ad hoc* set of rules allows the rejection of most of the false positives that are associated with larger structures in the breast. Figure 11 shows the result of the complete analysis of the region in figure 1. In this region, only one or two likely calcifications

have been cut, and nearly all of the identified calcifications would be reasonable to a human observer.

Correspondence is determined geometrically. In projection mammography, a calcification falls on a line between the image of the calcification and the x-ray focal spot. Given two views, the intersection of two lines should give the location of the calcification; a third view is redundant. Realistically, the three lines are skew, due to patient motion, the finite size of the image, and uncertainty in the acquisition geometry.

We simultaneously solve the correspondence problem and the geometry problem. We assume that geometric uncertainty can be compensated for by shifts of the second and third images. For each shift, a count is made of the number of triples whose positions are consistent with being the shadow of a single calcification. The parameter space of shifts is searched to maximize the count. For each possible triplet, the calcification position is found by minimizing the sum of the squares of the distances to the three corresponding shadow-to-x-ray-focus lines. The distance, δ^2 , calculated for each possible triplet, is sorted in ascending order so that each calcification image is used uniquely. The sum of $1/(1+(\delta^2/\Delta^2))^2$ is calculated over all remaining triplets. The result is a quantity which is 1 if the three shadows are in perfect agreement ($\delta^2=0$) and becomes 0 if the corresponding lines are highly skew (large δ^2). The value of Δ^2 is related to the distance between the best fit spatial points and the corresponding lines when these shadows are consistent. For this work Δ^2 is such that the distance of the best fit is 0.005 cm (the pixel pitch of the detector). An example of this calculation is shown in figure 12.

3. Results and Discussion

The segmentation and correspondence algorithms have proven to be quite robust. The segmentation algorithm results in far more calcifications per image being segmented than with human observers. On average, the human observer segmented 15.9 calcifications per image in a search for "all" calcifications; the current algorithm averaged 58 calcifications per image. However, as expected, the pairing algorithm markedly reduces the number of calcification candidates in the final 3-D image. In 120 cases, a human observer segmented and paired 9.0 calcifications per case. The computer algorithm paired 8.7 calcifications per case. Currently, only 48% of pairings match those of the human observer for cases of 8 or more calcifications. We have identified several reasons for this discrepancy. First, on review of the images, some pairings appear to be legitimate and missed by the human observer. Currently, we also miss those pairings in which calcifications are visible in only two views. Finally, not all calcifications are being segmented. Quantitative evaluation of the algorithms is ongoing, and concomitant refinements are being pursued. However, for the first time, we have been able to robustly and automatically generate 3-D images of breast calcifications.

References

1. A.D.A. Maidment, M. Albert, E.F. Conant, and S.A. Feig. 3-D Mammary Calcification Reconstruction from a Limited Number of Views. In *Physics of Medical Imaging*, Proceedings of the SPIE, **2708**, 378-389, (1996).
2. A.D.A. Maidment, M. Albert, and E.F. Conant. Three-Dimensional Imaging of Breast Calcifications. In *Exploiting New Image Sources and Sensors*. Proceedings of the SPIE, **3240**, 200-208 (1997).

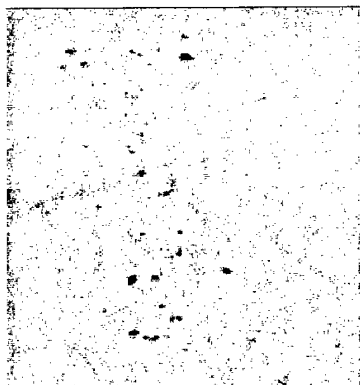


Figure 1: A calcified lesion after preliminary processing

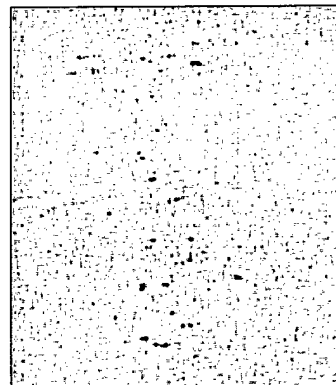


Figure 2: Laplacian operator applied to data from fig. 1

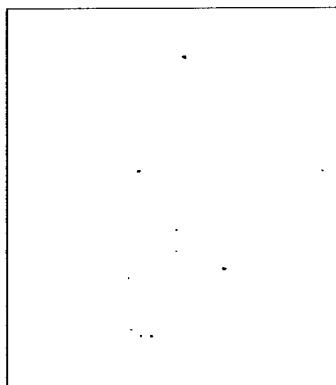


Figure 3: Threshold for fig. 2 which accepts too few pixels

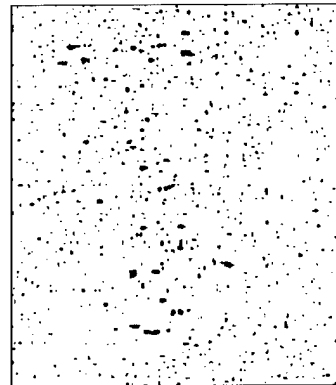


Figure 4: An appropriate threshold applied to fig. 2

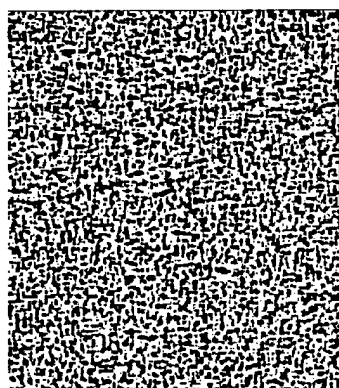


Figure 5: Threshold for fig. 2 which accepts too many pixels

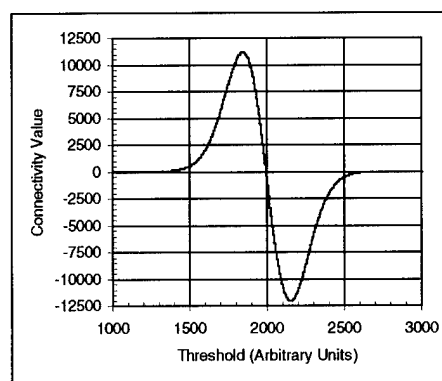


Figure 6: Connectivity factor for data in fig. 2 as a function of threshold



Figure 7: Calcification candidates for image using threshold in fig. 4

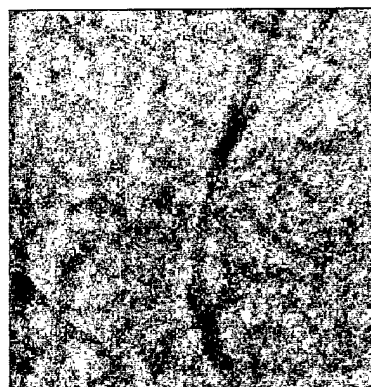


Figure 8: A sample region showing false positive candidates



Figure 9: Approximate segmentation of parenchymal structures

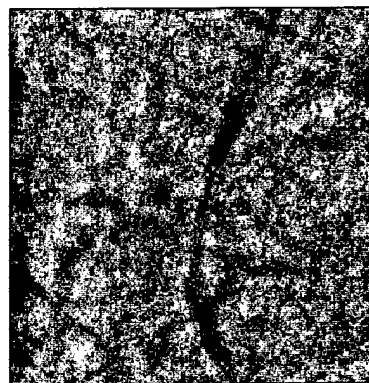


Figure 10: Remaining calcification candidates

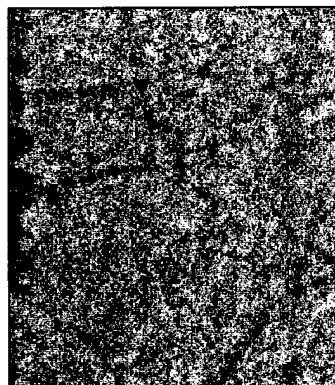


Figure 11: Final set of calcified regions from fig. 1

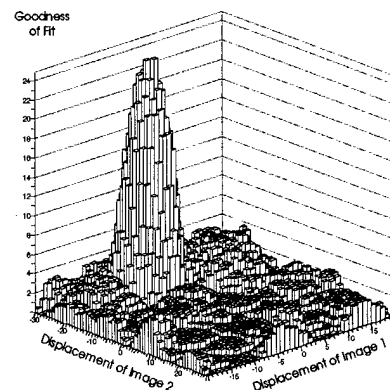


Figure 12: Goodness of fit parameter used for correspondence and motion correction